Energy & Buildings 166 (2018) 165–177

Contents lists available at ScienceDirect

Energy & Buildings

journal homepage: www.elsevier.com/locate/enbuild

Techno-economic analysis on frosting/defrosting operations for an air source heat pump unit with an optimized multi-circuit outdoor coil

Mengjie Song[a], Chiyan Tso[b,c,*], Christopher Yuhang Chao[b], Chili Wu[b,d]

[a] Department of Human and Engineered Environmental Studies, Graduate School of Frontier Sciences, The University of Tokyo, Japan
[b] Department of Mechanical and Aerospace Engineering, The Hong Kong University of Science and Technology (HKUST), Kowloon, Hong Kong
[c] HKUST Jockey Club Institute for Advanced Study, The Hong Kong University of Science and Technology, Hong Kong
[d] Building Energy Research Center, Guangzhou HKUST Fok Ying Tung Research Institute, Guangzhou, China

ARTICLE INFO

Article history:
Received 13 May 2017
Revised 4 January 2018
Accepted 28 January 2018
Available online 14 February 2018

Keywords:
Air source heat pump
Frosting/defrosting operation
Multi-circuit outdoor coil
Payback period
Techno-economic analysis

ABSTRACT

Air source heat pump (ASHP) units are used in applications around the world. After optimizing the multi-circuit outdoor coil by installing water collecting trays between circuits and adjusting the refrigerant distribution by using valves located at each circuit, system frosting/defrosting operation performances could be effectively improved. Before practical industry-scale application of trays and valves, their economic performances should be evaluated. However, in current literature, techno-economic analysis on operation performance of ASHP units is rare, which limits the development of innovative technologies. Therefore, a techno-economic analysis on frosting/defrosting operations is carried out in this study. Firstly, the frosting/defrosting experiments are introduced, followed by a series of assumptions and calculations. Then, the economic analysis results are provided in detail. Compared with a traditional ASHP unit, the total running costs of the modified unit in the heating season could save as much as 3681.75 CNY, or 10.33%, and the total cost decreased by 3516.75 CNY, or 4.67%, over 15 years of service life. The payback period of the additional initial cost is less than 8 months. Contribution of this work plays an important role in the evaluation and application of new technologies in the HVAC field.

1. Introduction

In recent decades, air source heat pump (ASHP) units have been used in applications worldwide due to their advantages of being highly efficient, environmentally friendly, low cost, easy to modify, etc. From a global point of view, over 90% of the world's population resides in regions where ASHP units can be suitably used for indoor thermal environmental control [1]. However, when an ASHP unit operates for space heating at a low temperature in a high humidity environment, frost will form and accumulate on the tube/fin surface of its outdoor coil. Frost becomes problematic, because it reduces the airflow passage area and acts as a thermal insulator, leading to performance degradation of the outdoor coil or even an unexpected shutdown of the ASHP unit [2]. Therefore, periodic defrosting becomes necessary.

There are many defrosting methods reported for ASHP units, such as compressor shutdown [3], electric heating [4], hot water spray [5], hot gas bypass [6], compressed air blowing [7], and ultrasonic defrosting [8], etc. Reverse cycle defrosting (RCD) is the most widely used, due to its advantages of easy adjustment, low energy and floor space consumption, high system safety and stability [9]. To further improve the RCD performance, different studies were conducted, including heating/dehumidifying the inlet air of the outdoor coil [10,11], structure adjustment or fin surface treatment [12–15], additional defrosting energy supply with phase change materials (PCMs) [9,16], frosting evenness value (FEV) improvement [17,18], and optimization of control strategies via refrigerant distribution adjustment [19–21], etc.

On the other hand, for an ASHP outdoor coil, a multi-circuit structure is usually used in order to enhance its heat transfer and minimize its refrigerant pressure loss [2,13,14,16–21]. To save floor space, it is always vertically installed, whereby the negative effects of melted frost flowing downwards along the tube surface due to gravity were experimentally and numerically demonstrated [9,13,14,22]. To alleviate the negative effects, water collecting trays were designed and installed under each circuit. Thus, the melted frost was taken away during defrosting, before it flowed downwards into the lower circuit(s) [13,14]. In addition, to optimize the frosting performances of an ASHP unit, a series of valves were used, located at the entrance and exit of each circuit, to improve the FEVs by adjusting the refrigerant distribution [17–19]. The un-

* Corresponding author at: Department of Mechanical and Aerospace Engineering, The Hong Kong University of Science and Technology (HKUST), Kowloon, Hong Kong.

E-mail address: mecytso@ust.hk (C. Tso).

https://doi.org/10.1016/j.enbuild.2018.01.060
0378-7788/

Nomenclatures

Variable	description unit
C_{ASHP}	initial cost of an ASHP unit (CNY)
$C_{e,\ unit}$	unit price of electricity (CNY/kWh)
$C_{f,\ i}$	total initial cost of the new ASHP unit in Case i (i = D1 – D8) (CNY)
$C_{f,\ T}$	initial cost of trays (CNY)
$C_{f,\ V}$	initial cost of valves (CNY)
$C_{i,\ V}$	installation cost of valves (CNY)
$C_{i,\ T}$	installation cost of trays (CNY)
$C_{r,\ C}$	total running cost in cooling season (CNY)
$C_{r,\ comp,\ DF}$	running cost of compressor during defrosting (CNY)
$C_{r,\ comp,\ F}$	running cost of compressor during frosting (CNY)
$C_{r,\ DF}$	running cost during defrosting operation (CNY)
$C_{r,\ F}$	running cost during frosting operation (CNY)
$C_{r,\ FDH}$	total running cost in heating season with frost formation (CNY)
$C_{r,\ ITE,\ DF}$	corresponding electricity cost of indoor air thermal energy consumed during defrosting operation (CNY)
$C_{r,\ id,\ fan,\ DF}$	running cost of indoor air fan during defrosting (CNY)
$C_{r,\ od,\ fan,\ DF}$	running cost of outdoor air fan during defrosting (CNY)
COP_C	system COP during cooling operation dimensionless
COP_{DF}	system COP during defrosting operation dimensionless
COP_F	system COP during frosting operation dimensionless
$P_{ave,\ od,\ fan}$	average power consumption of outdoor air fan during frosting (kW)
P_C	compressor power consumption during cooling operation (kW)
P_{DF}	compressor power consumption during defrosting operation (kW)
P_F	compressor power consumption during frosting operation (kW)
P_H	compressor power consumption during heating operation (kW)
$P_{id,\ fan}$	power consumption of indoor air fan (kW)
$P_{od,\ fan}$	power consumption of outdoor air fan (kW)
$Q_{id,\ air,\ C}$	indoor air thermal energy taken away during cooling operation (kJ)
$Q_{id,\ air,\ DF}$	indoor air thermal energy consumed during defrosting operation (kJ)
$Q_{id,\ air,\ F}$	indoor air thermal energy supplied during frosting operation (kJ)
T_{CD}	duration of cooling season in a year (day)
T_{DC}	duration of a frosting/defrosting cycle (minute)
T_{DD}	duration of defrosting operation in a cycle (minute)
T_{DF}	duration of frosting operation in a cycle (minute)
T_{FDH}	duration of heating season with frost formation in a year (day)
$T_{ind,\ in}$	average measured air temperature at the inlet of indoor coil °C
$T_{ind,\ out}$	average measured air temperature at the outlet of indoor coil °C
T_{NFDH}	duration of heating season without frost formation in a year (day)
T_{ODC}	system operating duration in a day in cooling season (hour)
T_{ODH}	system operating duration in a day in heating season without frost formatio (hour)
T_{OT}	operating cycle times in a day (time)
T_Y	service life of an ASHP unit (year)
$V_{i,\ air}$	volumetric flow rate of air passing through the indoor coil m^3/s
$\rho_{i,\ air}$	density of air in the indoor heated space kg/m^3

even defrosting phenomenon was also eliminated by the defrosting operation starting at a higher FEV, which results in a higher defrosting evenness value and better system defrosting performance [17,18]. However, the total initial purchase cost of the optimized ASHP unit would be increased by the additional investment of trays and valves, thus prolonging the predicted payback period.

For a new technology or innovation, a techno-economic analysis is very important and always given before scaling up to wider applications. In the literature, techno-economic analyses are easy to find in the fields of space heating systems [23–25], space cooling systems [26–28], hybrid heating and cooling systems [29–31], and renewable energy systems [32,33]. In particular, Horton et al. gave an economic analysis when they evaluated a high performance cold climate heat pump [34]. As reported, the maximum additional initial cost of the system changes for the Minneapolis location (USA), was $430 for a vapor injected system and $391 for an oil flooded system. These estimates assumed a 3-year simple payback period which was accepted by the customer. Moreover, Dong et al. experimentally studied an ASHP unit with a PCM thermal energy storage system added to improve its RCD performance [16], with its economic aspect separately discussed. Compared with a traditional unit, before the replacement of the PCMs, the running cost could save approximately 650 CNY over 7 years of service life.

However, although many methods were used to improve the operating performance of an ASHP unit, there is scarce reporting of techno-economic analysis on them. Previous studies [13,14,17–19] mainly focused on the energy aspect. There may be several reasons for this. Firstly, the technology or innovation is not mature or stable enough for the application, such as poor durability of some surface treatment methods [15]. Secondly, additional initial cost is too high, such as air dehumidification system for frost retarding [11]. Thirdly, the operation cycle is only partly considered, neglecting the heating operating performance, for example, when investigating system defrosting [15]. Fourthly, most researchers focused on the technology itself, or macroscopic energy policy. Clearly, there is a long way to go before these energy performance improvement measures are applied to ASHP units.

Therefore, to analyze the economic performance of the optimized ASHP unit with water collecting trays and/or valves installed in its multi-circuit outdoor coil, an economic analysis of its novel frosting/defrosting operation is conducted in this study. This study is helpful to guide new technologies and evaluate their industry-scale applications. Conclusions given in this study can also play a role in the pricing or governmental subsidy policy for ASHP units.

2. Methodology

Methodology of this economic analysis work is firstly illustrated in Fig. 1. As shown, the first step was an experimental study on an ASHP unit with a specially made three-circuit outdoor coil. Then, four typical conditions were designed, considering the installation style of trays and valves. After the experimental procedures were confirmed, a series of experiments were undertaken

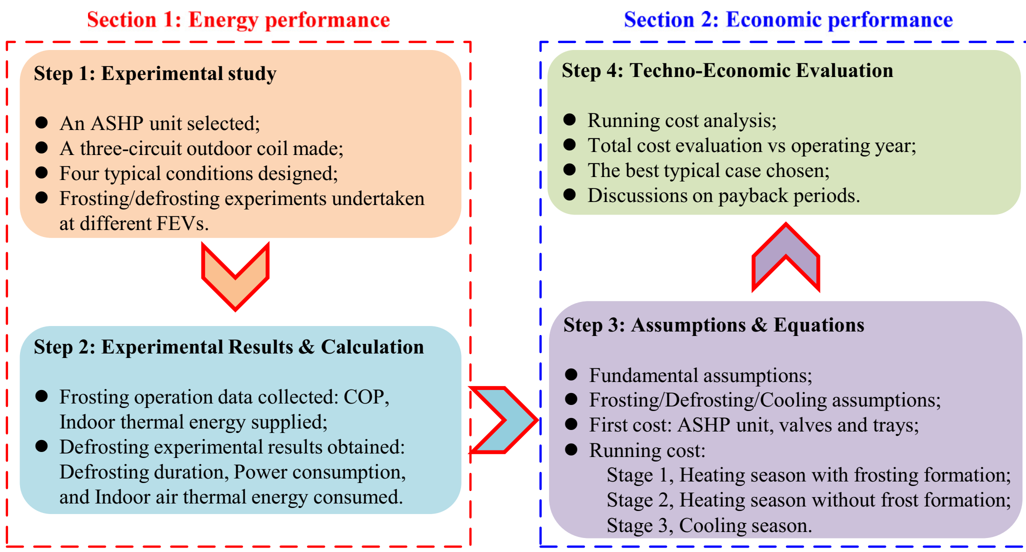

Fig. 1. Flow chart for the methodology used in this study.

Table 1
Parameters of the selected ASHP unit in this study.

Item	Parameters	Value	Unit
1	Rated cooling capacity	5.2	kW
2	Rated heating capacity	6.5	kW
3	Rated cooling power consumption	1600	kW
4	Rated heating power consumption	1840	kW
5	Rated cooling COP	3.25	–
6	Rated heating COP	3.53	–
7	Total price in Guangzhou, China	8000	CNY

Table 2
Two frosting experimental cases.

Item	Parameters	Case F1	Case F2
1	Valves (status)	With (fully open)	With (evenly adjusted)
2	Water collecting trays	With	With
3	FEV of outdoor coil	FEV_1 (< 100%)	FEV_2 (≈100%)
4	Frosting duration	60 min	60 min

with frost accumulated at different FEVs. Then, these experimental results and calculations, such as the coefficient of performance (COP), indoor air thermal energy supplied during frosting operation, and defrosting duration, etc., were collected and used in later techno-economic evaluations. The third step was the development of equations, including the first and subsequent running costs at different operating stages. After a series of conditions were assumed, the fourth step, a Techno-Economic Evaluation, is given. Finally, the techno-economic analysis on frosting/defrosting operations for optimized ASHP units is undertaken. The energy performance analysis, working as the basis of this study, is shown in Section 1. The economic performance was analyzed in Section 2, which is the focus of this study.

2.1. Experimental study

2.1.1. Experimental setup

An experimental ASHP unit was specifically designed for carrying out the experimental work illustrated in Fig. 1. The selected ASHP unit was a split-type that consisted of a swing type compressor, an accumulator, a four-way valve, an electronic expansion valve, an indoor coil and an outdoor coil. It was modified from a commercial variable speed Daikin ASHP unit, with its' performance parameters listed in Table 1. In the experimental ASHP unit, the indoor coil used was the prototype, with its model name of FTXD50FVM. However, considering the effects of trays and valves, a three-parallel refrigerant circuit outdoor coil was specially designed and used. As shown in Fig. 2, three solenoid valves (SVs) and three manual stop valves (MVs) were installed at the entrance and exit of each circuit in the outdoor coil. The solenoid valves stop the refrigerant flowing into/out of a circuit, and the manual stop valves were used to adjust the flow rates. Using this method, the frost accumulation on the surface of a circuit could be changed, and thus the FEV of a multi-circuit outdoor coil can be improved [19]. In addition, under each circuit, water collecting trays were used to collect the melted frost. After the frost that accumulated on the surface of each circuit melts, the water flows into a measuring cylinder, which was connected with the corresponding tray. Thus, the collected melted frost could be weighed and calculated. With this method, as reported in previous energy studies [13,14,17–19], the frosting/defrosting operation performances of an ASHP unit could be effectively improved.

2.1.2. Experimental case studies

The experimental ASHP unit was installed in an existing environmental chamber having a simulated heated indoor space and a simulated outdoor frosting space. The indoor and outdoor environment was controlled by the DX A/C system and two load generating units. The three-circuit outdoor coil was installed in the outdoor frosting space, where the frosting/defrosting cycle operations were carried out. Detailed experimental procedures and conditions were reported in References [17,20,22]. In a frosting/defrosting cycle, the frosting operation occurred first. After installing the valves, the frosting performance could be effectively optimized. Therefore, frosting experiments should be first undertaken before defrosting experiments. As listed in Table 2, two frosting experimental cases were designed, with both valves installed. Two different FEVs, FEV_1 and FEV_2, were reached with valves fully open and evenly adjusted. In a frosting/defrosting cycle, the frosting duration was fixed at 60 min. Frosting operation performance of an ASHP unit at different FEVs could be obtained from the experiments. As the baseline for comparison, valves in Case F1 were fully open, and the FEV_1 was less than 100% due to the refrigerant and air being unevenly distributed. In Case F2, valves were evenly adjusted, giving an FEV_2 value of almost 100%. Thus, the effects of valves were obvious in both cases.

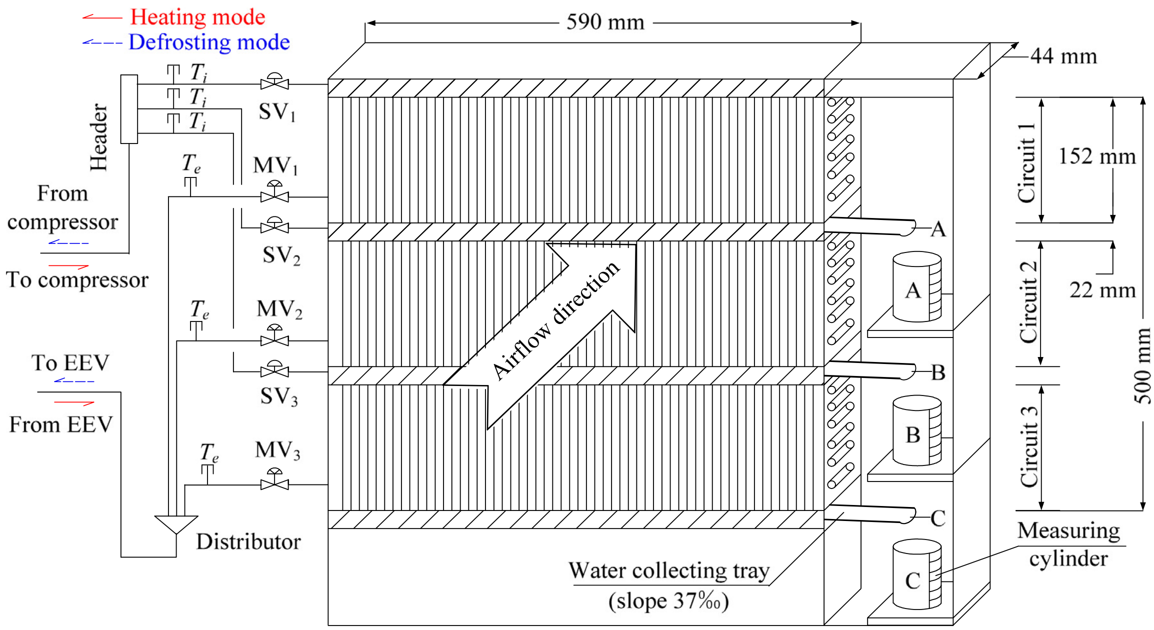

Fig. 2. Details of the three-parallel refrigerant circuit outdoor coil in this study [19].

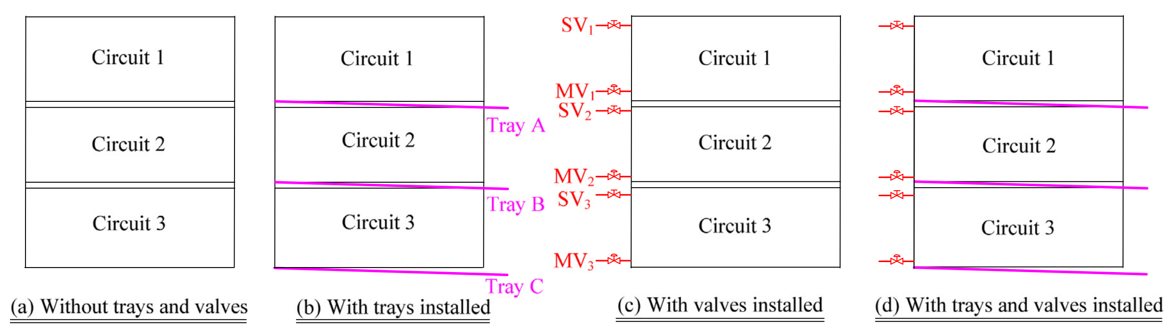

Fig. 3. Four typical conditions in this study.

Table 3
Four defrosting experimental cases.

Item	Parameters	Case D1	Case D2	Case D3	Case D4
1	Valves	Without	Without	With	With
2	Water collecting trays	Without	With	Without	With
3	Frosting duration	60 min	60 min	60 min	60 min
4	Cycle duration	70 min	70 min	70 min	70 min
5	FEV of outdoor coil	FEV_3	FEV_3	FEV_4	FEV_4
6	Shown in Fig. 3	(a)	(b)	(c)	(d)

The experimental results that form the basis for the economic analysis process in this study mainly came from previous defrosting experimental studies. Considering different installation styles of trays and valves, four typical defrosting conditions existed, as shown in Fig. 3. To compare, the prototype condition is shown in Fig. 3(a), without any change for an ASHP unit. In Fig. 3(b), trays were installed under each circuit, and thus the melted frost could be collected before it flowed downwards into the lower circuit(s). In this condition, the negative effects of downwards flowing melted frost could be eliminated. In Fig. 3(c), six valves were installed at the entrance and exit of the three circuits. In this condition, the FEV and DEV for the three-circuit outdoor coil could be adjusted [17–19]. However, in Fig. 3(d), both the trays and valves were installed. Four defrosting experimental cases were designed and listed in Table 3. In the defrosting experimental study, frosting duration was also designed at 60 min, and 70 min for a frosting/defrosting cycle. To keep the compressor safe, two periods of 3–4 min were left for its shut down. The durations in a cycle are illustrated in Fig. 4. Clearly, after installing the valves, the FEV should be higher at the start of defrosting operations. Therefore, FEVs were at FEV_3 and FEV_4 in the four defrosting experimental cases. FEV_4 was much higher than FEV_3. Here, FEV_3 and FEV_4 are the FEV values of the three-circuit outdoor coil at the start of defrosting without and with valves installed in each circuit, respectively.

2.1.3. Experimental results and analysis

Fig. 5 presents the airside surface conditions of the three-circuit outdoor coil at frosting operations in two experimental cases. Fig. 5(S1) and 5(S2) were at frosting after 10 min from the start, and Fig. 5(T1) and 5(T2) at their termination. It is obvious that frost accumulation in Case F2 was more even than that in Case F1. Frosting study shows that, when the opening degrees of valves were different, their FEVs changed. In Fig. 5, the FEV_1 was calculated at 75.7%, and the FEV_2 at 90.5%. Table 4 lists the experimental results. In Case F1, the average value of COP in 60 min was 4.10, with total indoor heat supplied 11,116 kJ. In Case F2, the two values were 4.26 and 11,543 kJ, respectively. In addition, average value of COP and total indoor heat supplied in the first 10 min were specially listed at 4.23 and 1922.6 kJ in Case F1, and 4.29 and 1942.4 kJ in Case F2, respectively. All the values in Case F1 were

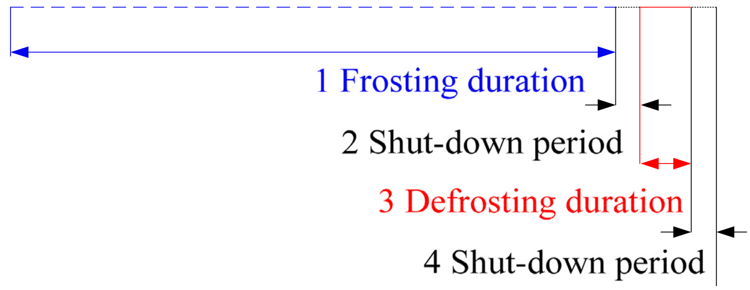

Fig. 4. Durations in a frosting/defrosting cycle in this experimental study.

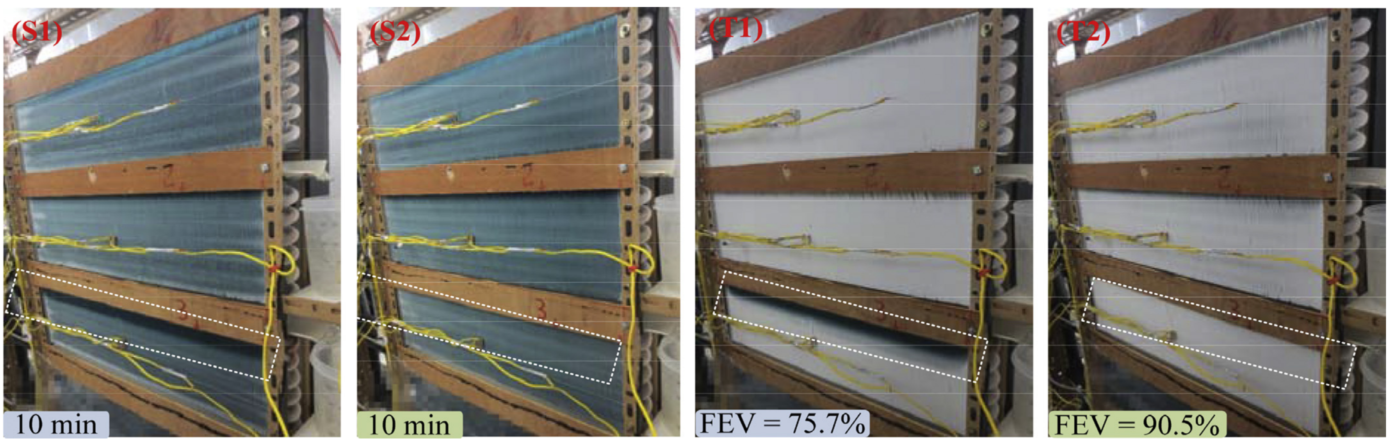

Fig. 5. Airside surface conditions of the three-circuit outdoor coil [22].

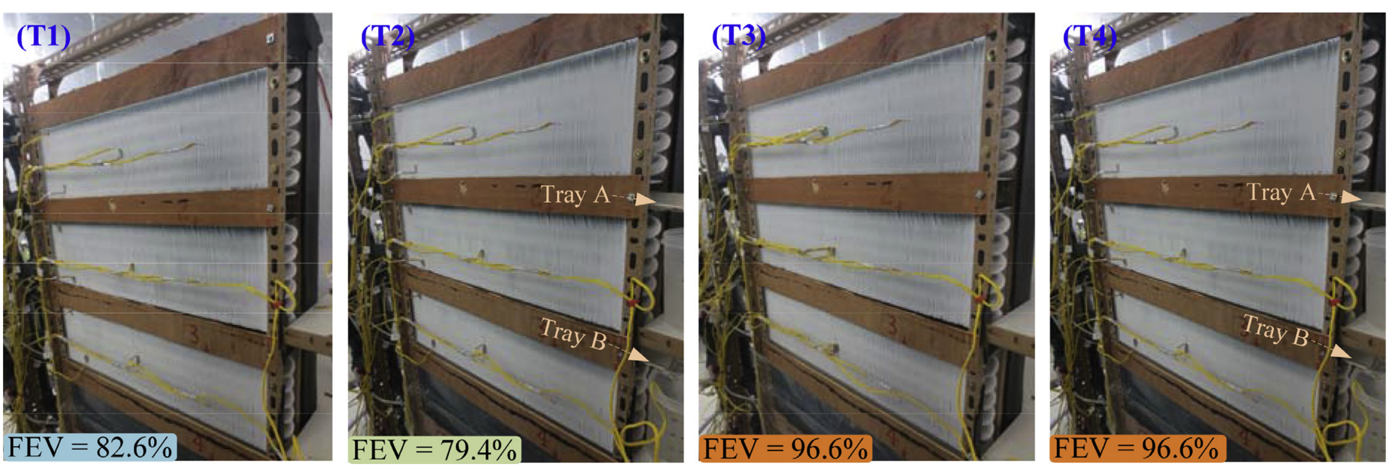

Fig. 6. Airside surface conditions at the start of defrosting in four cases [17,18].

Table 4
Experimental results of the two frosting cases.

Item	Parameters	Case F1	Case F2
1	Valves' status	Fully open	Evenly adjusted
2	FEV of outdoor coil	75.7%	90.5%
3	Average value of COP (60 min)	4.10	4.26
4	Average value of COP (first 10 min)	4.23	4.29
5	Indoor heat supplied (60 min)	11,116 kJ	11,543 kJ
6	Indoor heat supplied (first 10 min)	1922.6 kJ	1942.4 kJ
7	Conditions shown in Fig. 3	(a) and (b)	(c) and (d)
8	Results shown in Fig. 4	(S1) and (T1)	(S2) and (T2)

lower than those in Case F2. This data is used in the later calculations.

Different from Fig. 5, Fig. 6 shows the airside surface conditions at the start of defrosting for the three-circuit outdoor coil in four cases. Because no water collecting trays were placed under the circuits in Fig. 6(T1) and 6(T3), the effects of melted frost and FEV were coupled [17]. However, in Fig. 5(T2) and 5(T4), with trays installed to eliminate the effects of melted frost flowing downwards, only the effect of FEV on the defrosting performance was evaluated [18]. Due to the valves installed on each circuit, in Fig. 6(T3) and 6(T4), their FEVs were both at FEV_4, 96.6%. However, compared to the outdoor coil without valves installed, their defrosting started at lower FEVs, at 82.6% and 79.4% for Cases D1 and D2, respectively. Some experimental results are listed in Table 5. From Case D1 to Case D4, their total frost accumulations were 878 g, 1000 g, 881 g, and 969 g, respectively. The frosting duration was 60 min, but their defrosting durations were 205 s, 197 s, 185 s, and 175 s, respectively.

Table 5
Experimental results of the four defrosting cases.

Item	Parameters	Case D1	Case D2	Case D3	Case D4
1	FEV of outdoor coil	82.6%	79.4%	96.6%	96.6%
2	Total frost accumulation	878 g	1000 g	881 g	969 g
3	Defrosting duration	205 s	197 s	185 s	175 s
4	Total power inputs	124.6 kJ	128.0 kJ	107.6 kJ	117.3 kJ
5	Energy from indoor air	666.1 kJ	673.7 kJ	541.2 kJ	561.5 kJ
6	Condition shown in Fig. 3	(a)	(b)	(c)	(d)
7	Results shown in Fig. 6	(T1)	(T2)	(T3)	(T4)

To undertake this economic analysis work, total power inputs to compressor and indoor air fan, and thermal energy from the indoor air were calculated and presented.

2.2. Assumptions and calculation conditions

To analyze the economics of the frosting/defrosting operation performances, fundamental assumptions, frosting assumptions, defrosting assumptions, and cooling assumptions were given. The first type was assumed for all operating seasons, and the following three types for different operating seasons.

2.2.1. Fundamental assumptions

In this work, the following nine fundamental assumptions were firstly given:

i. Installation, running and maintenance costs of solenoid valves and the three-circuit outdoor coil on each circuit were neglected.
ii. Service life of an ASHP unit was assumed to be 15 years, and unit price of electricity at 0.9 CNY/kWh [16].
iii. In the whole service life of an ASHP unit, three operating seasons were divided: heating season with frost formation, heating season without frost formation, and cooling season.
iv. Durations of three operating seasons were constant, and assumed as climate conditions of Beijing city (Heating season: Nov. 15–Mar. 15 [35]).
v. In the heating season with frost formation, duration of a frosting/defrosting cycle was assumed at 70 min.
vi. In a frosting/defrosting cycle, frosting duration was fixed at 60 min, and two periods of 3–4 min for compressor shut down were left for its safety, as illustrated in Fig. 4; (To avoid an undesired shutdown for the ASHP unit, the frosting duration was not longer than 60 min in practical application.).
vii. Defrosting durations in four typical cases, system COP and defrosting efficiency were constant.
viii. All ambient air parameters, such as air temperature and relative humidity, were constant at fixed operating seasons.
ix. For the cases without valves installed, their FEVs were fixed at 75.7%. For the cases with valves installed, their FEVs were fixed at 96.6%.

2.2.2. Frosting assumptions

To calculate the running cost at frosting stage, system COP and indoor heat supplied should be obtained. Therefore, the following assumptions were also given.

i. Durations of heating season with frost formation and heating season without frost formation were both assumed to be 60 days/year.
ii. In heating season with frost formation, cycle operating was assumed to be 15 times/day. In heating season without frost formation, duration of frosting operating was assumed to be 12 h/day.

Table 6
Calculation data and experimental results of the two frosting cases.

Item	Parameters	Case F1	Case F3
1	Valves' status	Fully open	Evenly adjusted
2	FEV of outdoor coil	75.7%	96.6%
3	Average value of COP (60 min)	4.10	4.55
4	Average value of COP (first 10 min)	4.23	4.58
5	Indoor heat supplied (60 min)	11,116 kJ	11,719 kJ
6	Indoor heat supplied (first 10 min)	1922.6 kJ	1950.6 kJ
7	Conditions shown in Fig. 3	(a) and (b)	(c) and (d)

iii. When an ASHP unit works during the heating season with frost formation, system frosting COP was assumed at the average value of COP in 60 min, as listed in Item 3 in Table 4; (As presented in our previous work [36], when it reached 60 min, the COP decreased dramatically.).
iv. When the ASHP unit works during the heating season without frost formation, the system COP was assumed at the average value of COP in the first 10 min as listed in Item 4 in Table 4.
v. COP showed a good linear relationship with the FEV, allowing the values of COP at different FEVs to be calculated.
vi. Total indoor heat supplied showed a good linear relationship with the FEV. The values of indoor heat supplied at different FEVs could be calculated.

Based on the six assumptions and the data listed in Table 4, a series of experimental results in Case F3 were calculated and summarized in Table 6, with its FEV at 96.6%. Clearly, all the data in Case F3 were much bigger than those in Case F1 and Case F2. The COP and total indoor heat supplied at different stages listed in Table 6 would be used in the economic analysis.

2.2.3. Defrosting assumptions

To calculate the running cost at defrosting stage, the following five conditions were further assumed:

i. Defrosting duration showed a good linear relationship with the FEV, thereby, the defrosting durations at different FEVs could be calculated.
ii. Total power inputs to compressor and indoor air fan showed a good linear relationship with the FEV, allowing the values of total power inputs to compressor and indoor air fan at different FEVs to be calculated.
iii. Energy from indoor air showed a good linear relationship with the FEV, allowing the relative values at different FEVs to be calculated.
iv. FEV showed a good linear relationship with the total frost accumulation. Therefore, the FEVs could be calculated when the total frost accumulated changed.
v. Frost accumulation difference between Case D2 and Case D4, 31 g, was considered to have evaporated and was neglected.

Based on the five assumptions and the data listed in Table 5, a series of experimental results in the four typical cases were calculated. As listed in Table 7, results in Case D5 to Case D8 were based on the Case D1 to Case D4, respectively. In Cases D5 and D6,

Table 7
Calculation data and experimental results of the four defrosting cases.

Item	Parameters	Case D5	Case D6	Case D7	Case D8
1	FEV of outdoor coil	75.7%	75.7%	96.6%	96.6%
2	Total frost accumulation	1000 g	1000 g	969 g	969 g
3	Defrosting duration	245 s	202 s	203 s	175 s
4	Total power inputs	151.5 kJ	130.3 kJ	118.3 kJ	117.3 kJ
5	Total energy from indoor air	828.8 kJ	697.8 kJ	595.3 kJ	561.5 kJ
6	Condition shown in Fig. 3	(a)	(b)	(c)	(d)

their FEVs were changed from 82.6% and 79.4% to 75.7%. Clearly, defrosting duration, total power inputs, and energy from indoor air in Cases D5 and D6 were larger than those in Cases D1 and D2. In Cases D5, D7 and D8, their total frost accumulations were changed from 878 g, 881 g, and 969 g to 1000 g. At the same time, the defrosting duration, total power inputs to compressor and indoor air fan, and thermal energy from indoor air were calculated and listed in Table 7. All these data will be used in the economic analysis.

2.2.4. Cooling assumptions

Due to the trays and valves in cooling operation mode not being experimentally demonstrated, their running cost differences in the four typical cases were neglected. However, in the economic analysis work, all the cost during its operating life should be considered. Therefore, to calculate the running cost of the ASHP unit working in the cooling season, the following conditions were assumed:

i. Duration of cooling season was assumed to be 120 days/year, 12 h/day.
ii. System COP was assumed at the rated value, and Capacity of the ASHP unit at the rated cooling value, as listed in Table 1.

Based on the total 22 given assumptions in four types, the cost calculation equations used in the techno-economic analysis are given in the following section.

2.3. Economic analysis equations

2.3.1. Initial cost

Initial costs of three water collecting trays and six valves are $C_{f,\,T}$ and $C_{f,\,V}$, and their installation costs $C_{i,\,T}$ and $C_{i,\,V}$, respectively. The total initial cost of the new ASHP unit, $C_{f,\,i}$, covered the cost of an ASHP unit, C_{ASHP}, and the additional initial cost of trays and valves. They were separately evaluated by,

$$C_{f,D5} = C_{ASHP}, \tag{1}$$

$$C_{f,D6} = C_{ASHP} + C_{f,T} + C_{i,T}, \tag{2}$$

$$C_{f,D7} = C_{ASHP} + C_{f,V} + C_{i,V}, \tag{3}$$

$$C_{f,D8} = C_{ASHP} + C_{f,T} + C_{i,T} + C_{f,V} + C_{i,V}. \tag{4}$$

Initial cost of an ASHP unit was 8000 CNY, which was the same in the four typical cases. Additional initial cost of trays and valves was approximately 30 CNY and 300 CNY, respectively. The prices were relatively high because they were made-to-order for this study. However, if batch production of this equipment could be achieved, the additional initial costs of trays and valves are expected to be as low as 15 CNY and 150 CNY, respectively. Clearly, in Case D5, the total initial cost was the least, and in Case D8 the most. The biggest total additional initial cost, 165 CNY in Case D8, was only 2% of the initial cost of an ASHP unit.

2.3.2. Running cost

As shown in Fig. 7, the running costs of an ASHP unit in a year were calculated in three typical seasons (TSs). TS1 is heating season with frost formation, which contains frosting period and defrosting period. At the first period of TS1, TS2 and TS3, the running costs came from electricity consumption by the compressor, indoor and outdoor air fans. At the second period, the outdoor air fan was turned off. However, indoor air thermal energy would be consumed during defrosting, which came from the ambient air during frosting operation. Therefore, the corresponding electricity cost of indoor air thermal energy consumed was included. In Section 1, TS1 and TS2 are both in winter, which are different in four typical cases, due to their different energy performances. However, in Section 2, TS3 is in summer, which is the same in four typical cases, with their energy performances assumed to be constant.

TS1: Heating season with frost formation: In this typical season, the total running cost, $C_{r,\,FDH}$, includes three parts of electricity cost, (1) Electricity cost at frosting operation, $C_{r,\,F}$, (2) Electricity cost at defrosting operation, $C_{r,\,DF}$, and (3) Corresponding electricity cost of indoor air thermal energy consumed at defrosting operation, $C_{r,\,ITE,\,DF}$. This can be expressed as:

$$C_{r,FDH} = C_{r,F} + C_{r,DF} + C_{r,ITE,DF}, \tag{5}$$

where, electricity cost at frosting operation could be obtained by,

$$C_{r,F} = C_{r,comp,F} + C_{r,id,fan,F} + C_{r,od,fan,F}, \tag{6}$$

here, $C_{r,\,comp,\,F}$ was the running cost of the compressor at frosting operation:

$$C_{r,com,F} = C_{e,unit} \times P_F \times T_Y \times T_{FDH} \times T_{OT} \times T_{DF}. \tag{7}$$

In this equation, $C_{e,\,unit}$ is the unit price of electricity. P_F is the compressor power consumption at frosting operation, which could be tested in the experiment. In this study, the rated heating power consumption was 1840 kW, as listed in Table 1. T_Y was the service life of an ASHP unit, which is dominated by the level of maintenance work, and assumed at 15 years. In addition, the duration of heating season with frost formation in a year, $T_{FDH,}$ and the operating cycle times in a day, $T_{OT,}$ were assumed to be 60 days and 10 times, respectively. T_{DC} was the duration of a frosting/defrosting cycle. In Eq. (5), $C_{r,\,id,\,fan}$ and $C_{r,\,od,\,fan}$ are the running costs of indoor and outdoor air fans, which can be separately calculated by,

$$C_{r,id,fan} = C_{e,unit} \times P_{id,fan} \times T_Y \times T_{FDH} \times T_{OT} \times T_{DF}, \tag{8}$$

$$C_{r,od,fan} = C_{e,unit} \times P_{od,fan} \times T_Y \times T_{FDH} \times T_{OT} \times T_{DF}. \tag{9}$$

However, during frosting operation of an ASHP unit, the frost accumulated on the surface of the outdoor coil, adversely affects the capacity of the outdoor air fan [13,14]. Therefore, the running cost of the outdoor air fan was always calculated by,

$$C_{r,od,fan} = C_{e,unit} \times P_{ave,od,fan} \times T_Y \times T_{FDH} \times T_{OT} \times T_{DF}, \tag{10}$$

where, $P_{ave,\,od,\,fan}$ is the average power consumption of the outdoor air fan, which could be tested in the experimental study. Then, us-

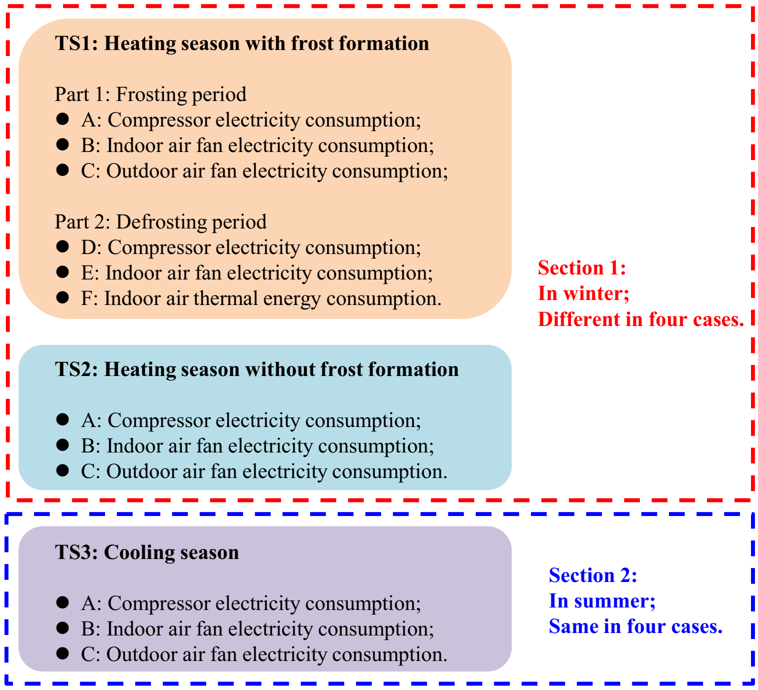

Fig. 7. Running costs of ASHP unit in three typical seasons of a year.

ing Eqs. (6)–(8) and (10), the total electricity cost during the frosting operation was,

$$C_{\mathrm{r,F}} = C_{e,unit} \times (P_f + P_{id,fan} + P_{ave,od,fan}) \times T_Y \times T_{FDH} \times T_{OT} \times T_{DF}. \tag{11}$$

In this study, the $C_{r,\,F}$ was also calculated by,

$$C_{\mathrm{r,F}} = \frac{Q_{id,air,F}}{COP_F}, \tag{12}$$

where, $Q_{id,\,air,\,\mathrm{F}}$ was the indoor air thermal energy supplied at frosting operation, or the rated heating capacity, at 6.5 kW, listed in Table 1. COP_F was the system COP at frosting operation, which could be calculated at Section 2.2.2 using the relative FEVs. Further, in Eq. (5), the running cost of defrosting operation, $C_{r,\,DF}$, covered the running costs of compressor and indoor air fan. It was,

$$C_{\mathrm{r,DF}} = C_{r,comp,\mathrm{DF}} + C_{r,id,fan,DF}. \tag{13}$$

In this equation, different from the $C_{r,\,comp,\,f}$ in Eq. (6), the running cost of the compressor during defrosting, $C_{r,\,comp,\,\mathrm{DF}}$, was evaluated by,

$$C_{r,comp,\mathrm{DF}} = C_{e,unit} \times P_{DF} \times T_Y \times T_{FDH} \times T_{OT} \times T_{DD}, \tag{14}$$

where, the defrosting power consumption of the compressor, P_{DF}, and duration of defrosting in a cycle, T_{DD}, were changing with the working conditions. In this period, the electricity cost of the indoor air fan was given by,

$$C_{r,id,fan,DF} = C_{e,unit} \times P_{id,fan} \times T_Y \times T_{FDH} \times T_{OT} \times T_{DD}. \tag{15}$$

Thus, using Eqs. (13)–(15), the following equation yields,

$$C_{\mathrm{r,DF}} = C_{e,unit} \times (P_{DF} + \mathrm{P}_{id,fan}) \times T_Y \times T_{FDH} \times T_{OT} \times T_{DD}. \tag{16}$$

However, the electricity cost at defrosting operation, $C_{r,\,DF}$, was calculated by Eq. (13). In this equation, the electricity consumption data of the compressor and indoor air fan were collected in experimental study, which are listed in Table 7. Finally, in Eq. (5), the corresponding electricity cost of indoor air thermal energy consumed at defrosting operation, $C_{r,\,ITE}$, was evaluated by,

$$C_{r,ITE} = \frac{Q_{id,air,DF}}{COP_F}. \tag{17}$$

The COP_F can be calculated during frosting operation by,

$$COP_{\mathrm{F}} = \frac{Q_{id,air,F}}{(P_{comp} + P_{id,fan} + P_{aver,od,fan}) \times T_{DF}}. \tag{18}$$

Here, the indoor air thermal energy supplied at frosting operation, $Q_{id,\,air,\,F}$, is:

$$Q_{id,air,F} = c_{i,air} m_{i,air} \Delta t = c_{i,air} \rho_{i,air} V_{i,air} (T_{\mathrm{ind,in}} - T_{ind,out}), \tag{19}$$

where $\rho_{i,\,air}$ is the density of air in the indoor heated space, $V_{\mathrm{i,\,air}}$ the volumetric flow rate of air passing through the indoor coil, $T_{\mathrm{ind,\,in}}$ and $T_{\mathrm{ind,\,out}}$ the average values of measured air temperatures at the inlet and outlet of the indoor coil. All parameters were obtained in the experiments, as well as the indoor air thermal energy consumed at defrosting operation, $Q_{id,\,air,\,DF}$ in Eq. (17). Considering Eqs. (5), (11), (16), and (17), the total running cost of an ASHP unit in the heating season with frost formation is:

$$\begin{aligned} C_{r,FDH} = {} & C_{e,unit} \times T_Y \times T_{FDH} \times T_{OT} \times [(P_f + P_{id,fan} + P_{ave,od,fan}) \times T_{DF} \\ & + (P_{DF} + P_{id,fan}) \times T_{DD}] + \frac{Q_{id,air,DF}}{\mathrm{COP_F}}. \end{aligned} \tag{20}$$

However, in this study, it was evaluated by Eqs. (5), (12), (13) and (17):

$$C_{r,FDH} = \frac{Q_{id,air,F} + Q_{id,air,DF}}{\mathrm{COP_F}} + \mathrm{C}_{r,comp,DF} + C_{r,id,fan,DF}. \tag{21}$$

TS2: Heating season without frost formation: When an ASHP unit works in the heating season without frost formation, the total running cost, $C_{r,\,NFDH}$, includes three parts of electricity cost, (1) electricity cost of compressor, $C_{r,\,\mathrm{comp},\,\mathrm{h}}$, (2) electricity cost of indoor air fan, $C_{r,\,id,\,fan}$, and (3) electricity cost of outdoor air fan, $C_{r,\,od,\,fan}$:

$$C_{\mathrm{r,NFDH}} = C_{r,comp,NFDH} + C_{r,id,fan} + C_{r,od,fan}. \tag{22}$$

In this equation, the three unknown parameters can be calculated by,

$$C_{r,comp,\mathrm{NFDH}} = C_{e,unit} \times P_{NFDH} \times T_Y \times T_{\mathrm{NFDH}} \times T_{ODH}, \tag{23}$$

$$C_{r,id,fan} = C_{e,unit} \times P_{id,fan} \times T_Y \times T_{NFDH} \times T_{ODH}, \tag{24}$$

$$C_{r,od,fan} = C_{e,unit} \times P_{od,fan} \times T_Y \times T_{NFDH} \times T_{ODH}, \tag{25}$$

In Eqs. (23)–(25), T_{ODH} is the system operating duration in a day in the heating season without frost formation, assumed to be 12 h. Considering Eqs. (22)–(25), the total running cost in the heating season without frost formation can be evaluated by,

$$C_{r,NFDH} = C_{e,unit} \times (P_{\mathrm{NFDH}} + P_{id,fan} + P_{od,fan}) \times T_Y \times T_{NFDH} \times T_{ODH}. \tag{26}$$

In this study, it was also evaluated by,

$$C_{r,\mathrm{NFDH}} = \frac{Q_{id,air,NFDH}}{COP_{NFDH}}, \tag{27}$$

where, the indoor air thermal energy supplied at the frosting operation and the system COP in this season, $Q_{id,\ air,\ NFDH}$ and $\mathrm{COP_{NFDH}}$, were also obtained from experiments.

TS3: Cooling season: The total running cost for an ASHP unit in the cooling season, $C_{r,\ C}$, consists of the electricity cost of the compressor, $C_{r,\ comp,\ C}$, electricity cost of the indoor air fan, $C_{r,\ id,\ fan}$, and electricity cost of the outdoor air fan, $C_{r,\ od,\ fan}$:

$$C_{r,C} = C_{r,comp,\mathrm{C}} + C_{r,id,fan} + C_{r,od,fan}. \tag{28}$$

In Eqs. (22) and (28), the three unknown parameters were evaluated by,

$$C_{r,comp,\mathrm{C}} = C_{e,unit} \times P_C \times T_Y \times T_{\mathrm{CD}} \times T_{ODC}, \tag{29}$$

$$C_{r,id,fan} = C_{e,unit} \times P_{id,fan} \times T_Y \times T_{\mathrm{CD}} \times T_{\mathrm{ODC}}, \tag{30}$$

$$C_{r,od,fan} = C_{e,unit} \times P_{od,fan} \times T_Y \times T_{\mathrm{CD}} \times T_{\mathrm{ODC}}, \tag{31}$$

In Eqs. (29)–(31), the system operating duration in the cooling season, T_{ODC}, was assumed to be 12 h. Using the three equations, the total running cost can be expressed as,

$$C_{r,\mathrm{C}} = C_{e,unit} \times (P_{\mathrm{C}} + P_{id,fan} + P_{od,fan}) \times T_Y \times T_{CD} \times T_{ODC}. \tag{32}$$

In this study, the total running cost in the cooling season was also obtained by,

$$C_{r,C} = \frac{Q_{id,air,C}}{COP_C}. \tag{33}$$

In the four typical cases, the indoor air thermal energy taken away during the cooling operation, $Q_{id,\ air,\ \mathrm{C}}$, was replaced by the rated cooling capacity of the ASHP unit, at 5.2 kW. At the same time, the system COP in the cooling season, $\mathrm{COP_C}$, also used the rated value at 3.25. The two values are both listed in Table 1.

2.3.3. Economic analysis model

Total running costs in four typical cases were:

$$C_{r,i} = C_{r,FDH,i} + C_{r,NFDH,i} + C_{r,C,i} \quad (i = D5,\ D6,\ D7,\ and\ D8). \tag{34}$$

Considering Eqs. (20), (26), (32) and (34), it can be evaluated by,

$$\begin{aligned} C_r = {} & C_{e,unit} T_Y \{ T_{FDH} T_{OT} [(P_F + P_{id,fan} + P_{ave,od,fan}) T_{DF} \\ & + (P_{DF} + P_{id,fan}) T_{DD}] + (P_H + P_{id,fan} + P_{od,fan}) T_{NFDH} T_{ODH} \\ & + (P_C + P_{id,fan} + P_{od,fan}) T_{CD} T_{ODC} \} + \frac{Q_{id,air,DF}}{\mathrm{COP_F}} \end{aligned}. \tag{35}$$

In this study, C_r was also calculated by Eqs. (21), (27), (33) and (34), as,

$$\begin{aligned} C_r = {} & \frac{Q_{id,air,F} + Q_{id,air,DF}}{\mathrm{COP_F}} + \frac{Q_{id,air,NFDH}}{\mathrm{COP}_{NFDH}} + \frac{Q_C}{\mathrm{COP}_C} \\ & + C_{r,comp,DF} + C_{r,id,fan,DF}. \end{aligned} \tag{36}$$

Therefore, the total costs in four typical cases were separately expressed as:

$$\begin{aligned} C_{r,\mathrm{D5}} = {} & \frac{Q_{id,air,F} + Q_{id,air,DF}}{\mathrm{COP_F}} + \frac{Q_{id,air,NFDH}}{\mathrm{COP}_{NFDH}} + \frac{Q_C}{\mathrm{COP}_C}, \\ & + C_{r,comp,DF} + C_{r,id,fan,DF} + C_{ASHP} \end{aligned} \tag{37}$$

$$\begin{aligned} C_{r,\mathrm{D6}} = {} & \frac{Q_{id,air,F} + Q_{id,air,DF}}{\mathrm{COP_F}} + \frac{Q_{id,air,NFDH}}{\mathrm{COP}_{NFDH}} + \frac{Q_C}{\mathrm{COP}_C}, \\ & + C_{r,comp,DF} + C_{r,id,fan,DF} + C_{ASHP} + C_{f,T} + C_{i,T} \end{aligned} \tag{38}$$

$$\begin{aligned} C_{r,\mathrm{D7}} = {} & \frac{Q_{id,air,F} + Q_{id,air,DF}}{\mathrm{COP_F}} + \frac{Q_{id,air,NFDH}}{\mathrm{COP}_{NFDH}} + \frac{Q_C}{\mathrm{COP}_C}, \\ & + C_{r,comp,DF} + C_{r,id,fan,DF} + C_{ASHP} + C_{f,V} + C_{i,V} \end{aligned} \tag{39}$$

$$\begin{aligned} C_{r,\mathrm{D8}} = {} & \frac{Q_{id,air,F} + Q_{id,air,DF}}{COP_F} + \frac{Q_{id,air,NFDH}}{COP_{NFDH}} + \frac{Q_C}{COP_C} \\ & + C_{r,comp,DF} + C_{r,id,fan,DF} + C_{ASHP} + C_{f,T} + C_{i,T} + C_{f,V} + C_{i,V} \end{aligned}. \tag{40}$$

Based on all the listed assumptions and known experimental data, all the costs in four typical cases could be calculated with the 40 equations given in this Section.

3. Results and discussions

All the calculation results are shown in Figs. 8–13. Among them, the running costs of four typical cases are presented in Figs. 8–10, and total costs shown in Figs. 10 and 11. Proportions of initial cost and additional initial cost in the total cost are shown in Fig. 12. Variation of electricity unit price is discussed and presented in Fig. 13.

Fig. 8(a) shows the running costs of four typical cases in three typical seasons over 15 operating years. In the cooling season, the running costs are always the highest. This resulted from the operating duration this season being the longest, at 21,600 h. However, the operating duration in the heating season with frost formation was only 13,500–15,750 h, and that in the heating season without frost formation the shortest, at 10,800 h. In four typical cases, the running costs in the cooling season are same at 31,104 CNY. This is because of the effects the valves have on the system COP in this operating season were neglected. For the running cost in the heating season with frost formation, the differences in four typical cases were obvious due to the effects of the trays and valves. From highest to lowest, their values were 21251.46 CNY in Case D5, 20952.48 CNY in Case D6, 18758.5 CNY in Case D7, and 18711.1 CNY in Case D8. The largest difference between Cases D5 and D8 demonstrated that, the running cost of the ASHP unit in the heating season with frost formation could decrease by as much as 2540.36 CNY or 11.95%, after the trays and valves were installed. In addition, for the running cost in the heating season without frost formation, from Case D5 to Case D8, the values were 14936.17 CNY, 14936.17 CNY, 13794.8 CNY, and 13794.8 CNY, respectively. The effects of the water collecting trays on defrosting performance did not exist in this operating season. But the effect of the valves was shown, with the difference of 1141.37 CNY between Cases D5 and D8. It was demonstrated that, the running cost of the new ASHP unit in the heating season without frost formation could decrease by as much as 7.64%. Therefore, after optimizing the ASHP unit with trays and/or valves, its economic performance would be better.

To clearly compare the running costs in the heating season in four typical cases, Fig. 8(b) shows their running costs in a year. It is obvious that the running cost in the heating season without frost formation was much more than that in the heating season with frost formation. From highest to lowest, the running costs in the heating season with frost formation were 1416.76 CNY in Case D5, 1396.83 CNY in Case D6, 1250.57 CNY in Case D7, and 1247.41 CNY in Case D8. Their biggest

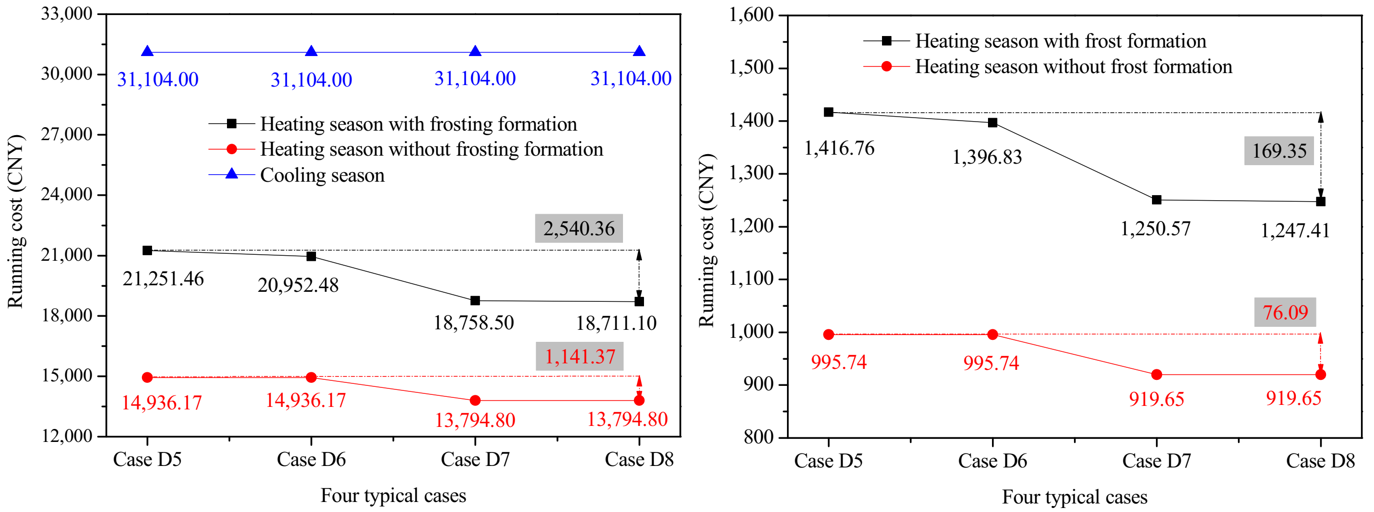

(a) Running costs in three typical seasons in the 15 operating years (b) Running costs in two heating seasons in 1 operating year

Fig. 8. Running costs over 15 and 1 operating years.

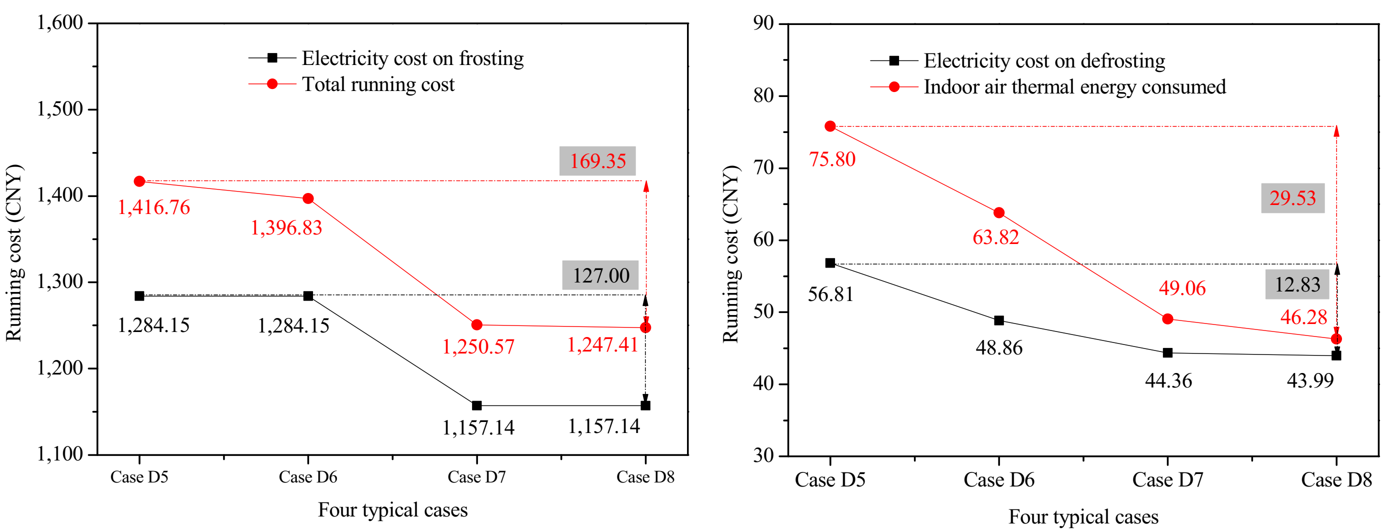

(a) Running costs in frosting in 1 operating year (b) Running costs in defrosting in 1 operating year

Fig. 9. Running costs in the heating season with frost formation in 1 operating year.

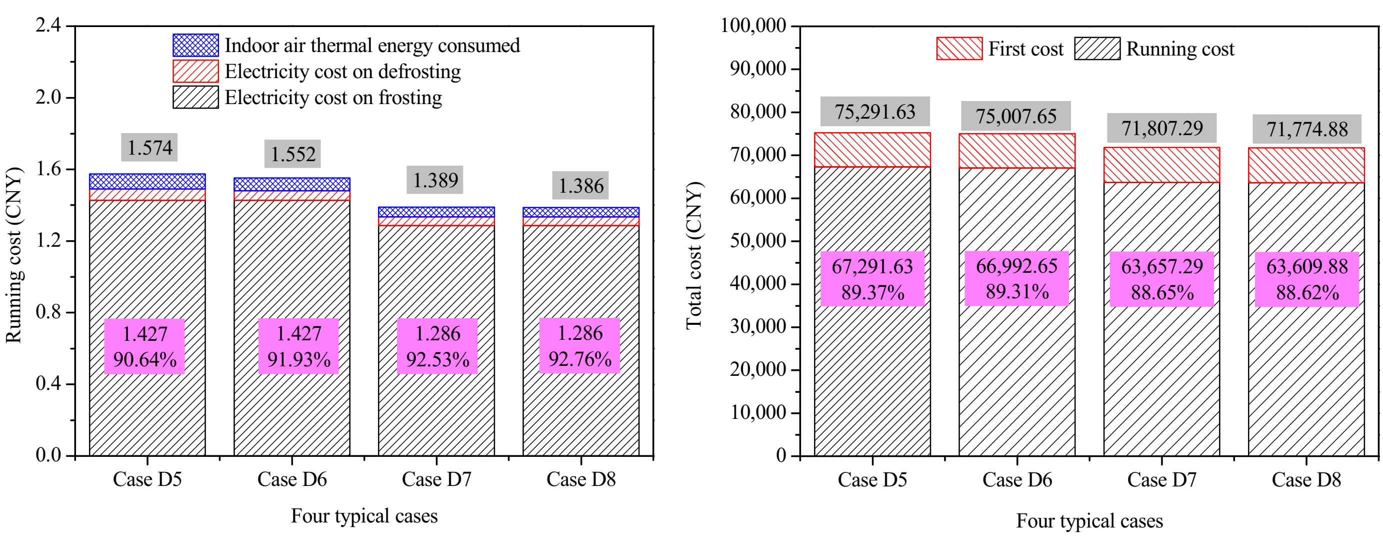

(a) Running costs in a frosting/defrosting cycle (b) Total costs in the four typical cases in 15 operating years

Fig. 10. Running costs and total costs in a cycle and 15 operating years.

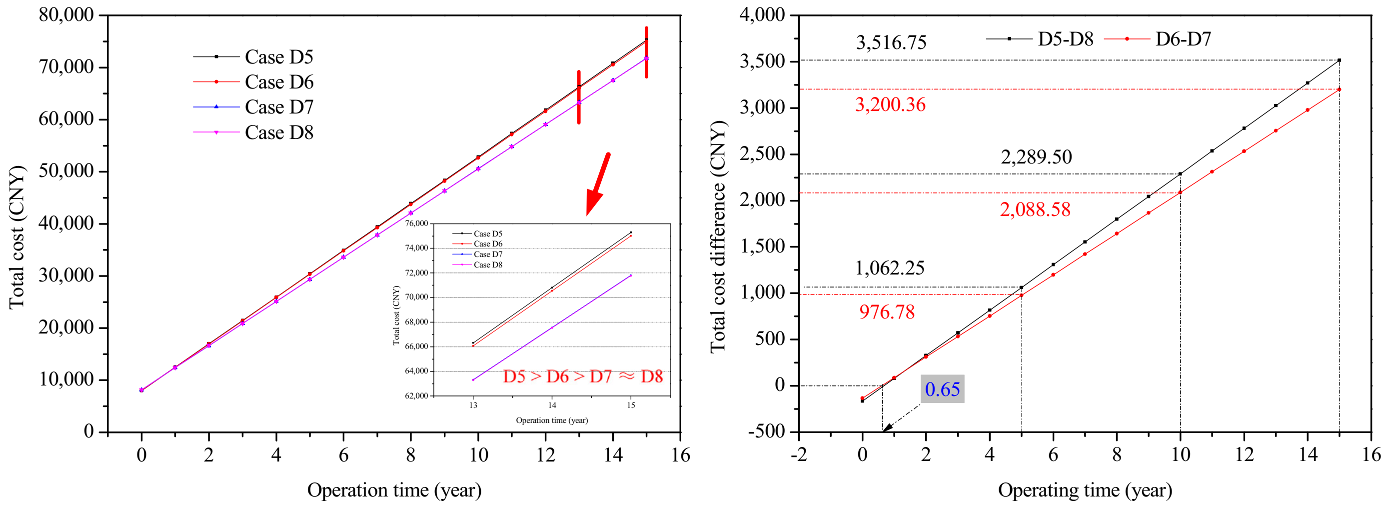

(a) Total costs in 15 operating years

(b) Total cost differences between four cases

Fig. 11. Total costs and their differences over 15 operating years.

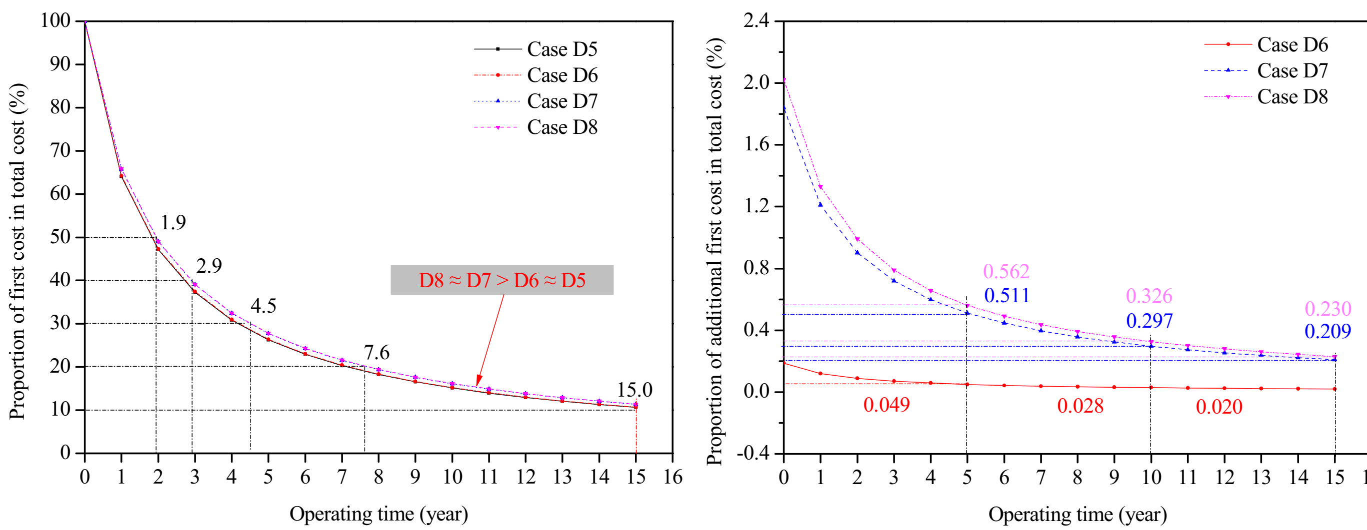

(a) Proportion of first cost in total cost

(b) Proportion of additional first cost in total cost

Fig. 12. Proportions of initial cost and additional initial cost of the total cost over 15 years.

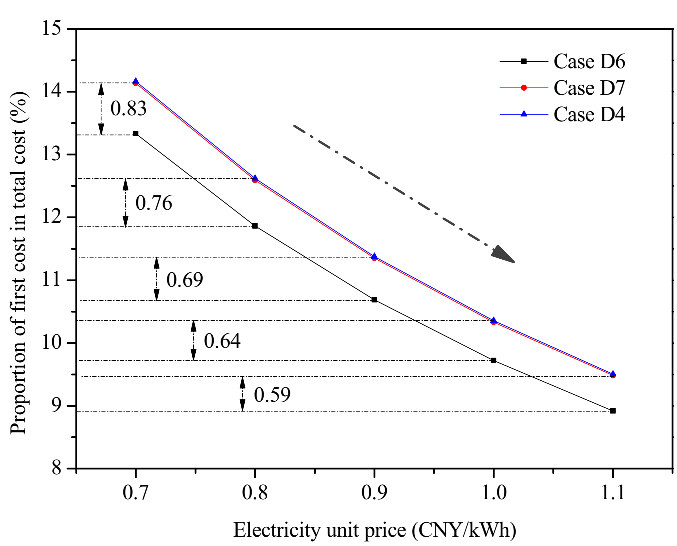

Fig. 13. Proportions of initial cost of the total cost with electricity unit price variation.

difference was 169.35 CNY between Case D5 and Case D8. For the running costs in the four typical seasons in the heating season without frost formation, their values were at 995.74 CNY in Cases D5 and D6, and 919.65 CNY in Case D7 and D8. Their biggest difference was also between Case D5 and Case D8, at 76.09 CNY, which was smaller than the difference in the heating season with frost formation. This is because the water collecting trays installed had no effect as there was no defrosting operation during the heating season without frost formation. In addition, the total difference showed that, after trays and valves were installed, the total running cost during heating seasons could decrease by 245.44 CNY, or 10.17%.

Furthermore, in order to clearly analyze the running cost consumed in the heating season with frost formation, Fig. 9 shows the running costs in four typical cases in a year. As shown in Fig. 9(a), the trends of the two curves are nearly the same. This shows that the total running cost was mainly decided by the electricity cost of the frosting operation stage. It is reasonable, because the operation duration frosting is 60 min during a 70 min period frosting/defrosting cycle. However, the total running cost shows at D5 > D6 > D7 > D8, but electricity cost on frosting at

D5 = D6 > D7 = D8. This is because the trays and valves had no effect at this stage. As shown in Fig. 9(b), these effects were shown on running costs of electricity on defrosting, and indoor air thermal energy consumed during defrosting. Therefore, from highest to lowest, the running cost was 1416.76 CNY in Case D5, 1396.83 CNY in Case D6, 1250.57 CNY in Case D7, and 1247.41 CNY in Case D8. Their biggest difference was 169.35 CNY between Case D5 and Case D8. Here, the fact that the running cost could save a lot after trays and valves were installed was further confirmed. Also, from the big difference between Case D6 and Case D7, as shown in Fig. 9(a), we can find that the economic effects of valves are bigger than those of trays. Due to the installation of trays and valves, in Fig. 9(b), the trends of the two curves show that, from Case D5 to Case D8, their running costs became steadily smaller. Their biggest difference was also shown between Case D5 and Case D8, at 29.53 CNY in indoor air thermal energy consumed, and 12.83 CNY in electricity cost during defrosting. It is interesting that the value of indoor air thermal energy consumed during the defrosting operation is always higher than the electricity cost of defrosting. This is because the cold refrigerant takes more thermal energy from the indoor air during defrosting. Clearly, the defrosting duration in Case D8 was the shortest. Therefore, the running cost in this case was always the lowest.

In order to analyze the proportions of three running costs, indoor air thermal energy consumed, electricity cost on defrosting and frosting stages, the data showing the running cost of a frosting/defrosting cycle in the heating season with frost formation is available in Fig. 10(a). In four typical cases, their total running costs are decreasing steadily from Case D5 to Case D8. Their values were 1.574 CNY in Case D5, 1.552 CNY in Case D6, 1.389 CNY in Case D7, and 1.386 CNY in Case D8. However, for the electricity cost during frosting in four cases, although their values show at D5 = D6 > D7 = D8, their proportions at D5 < D6 < D7 < D8. It is easy to conclude that, the running cost saved at the defrosting stage was much more than that saved at the frosting stage. This also reflects the economic performance of an ASHP unit was highly improved after the trays and valves were installed. Fig. 10(b) shows the total costs in the four typical cases over 15 operating years. From big to small, their values were at 64880.46 CNY in Case D5, 64716.08 CNY in Case D6, 63910.52 CNY in Case D7, and 63895.80 CNY in Case D8. This directly reflects that the economic performances of an ASHP could be effectively improved after trays or/and valves are installed. With nearly the same initial costs, the total costs in the four cases were mainly decided by their running costs. The running cost in Case D5 was 56880.46 CNY, but 55730.80 CNY in Case D8. That means that as much as 3681.75 CNY, or 5.47%, of the running cost could be saved after the trays and valves are installed, from conditions (a) to (d) shown in Fig. 3. With their initial costs considered, the total cost decreased by as much as 3516.75 CNY, or 4.67%.

Fig. 11(a) shows total costs in four typical conditions over 15 operating years. As the Fundamental Assumptions are given, the total costs kept increasing in line with the operating time. In practical application, the total running cost would increase much quicker than expected, because the energy performances of the ASHP unit would decrease with time. Also, the maintenance costs increase the total running cost. As shown in Fig. 11(a), the running cost relationship of four typical cases shows at D5 ≈ D6 > D7 ≈ D8. This also reflects the effects of valves were more obvious than that of trays on the running cost. After 2 years of operation, their differences were obvious. As shown in the inset in Fig. 11(a), their relationship became at D5 > D6 > D7 ≈ D8 after 12 years of operation. The running period enlarged their differences. Therefore, conclusions of this study play important roles in the budgeting work of equipment procurement. To clearly show the biggest difference of total costs in four typical cases, the difference between Cases D5 and D8 is further shown in Fig. 11(b). Also, to further confirm the effects of valves is larger than those of trays, the total cost difference between Case D6 and Case D7 in the 15 operating years is shown in this figure. When their values were 0, the operating periods were both at 0.65 year. That means their additional initial costs in Cases D6, D7 and D8 could be covered by their running costs in 0.65 year, compared with the total cost in Case D5. When the operating duration was 5, 10, or 15 years, the total costs saved could be as much as 1062.25 CNY, 2289.50 CNY, and 3516.75 CNY, respectively. Meanwhile, the total cost difference between installing trays and valves was 976.78 CNY, 2088.58 CNY, and 3200.36 CNY, respectively.

Fig. 12(a) shows proportions of the initial cost of the total cost in four typical cases over 15 operating years. At the end of its life span, their relationship showed at D8 ≈ D7 > D6 ≈ D5. This also confirmed the installation of trays and valves could save more money in an ASHP unit's application. As shown, when the recovery proportions of initial costs were at 50%, 40%, 30% and 20%, the operating durations were at 1.9, 2.9, 4.5, and 7.6 years, respectively. That means, before the ASHP unit works 8 years, more than 80% of the initial cost could be recovered. After 15 years, the initial cost becomes only 10% of the total cost. It is also confirmed that the total cost is mainly decided by the running cost. After the trays and valves are installed, the total cost could significantly decrease. To clearly show the additional initial cost effect on the total cost during operation of an ASHP unit, Fig. 12(b) shows proportions of the additional initial cost of the total cost over 15 operating years in three typical cases. As shown, the curve of Case D6 was the lowest, because its additional cost was the smallest, only 15 CNY for the three water collecting trays. Therefore, after the ASHP unit worked 5 years, 10 years, and 15 years, the proportions of the additional initial cost of the total cost remained very small, at only 0.409%, 0.028%, and 0.020%, respectively. However, the line of Case D8 was always the highest, because its additional initial cost was the most, 165 CNY for trays and valves. Although the proportions in Cases D7 and D8 were much bigger, when the ASHP unit worked for 5 years, additional initial costs became less than 0.6% of total cost. This also reflects the dominant role of running cost on economic analysis of an ASHP unit. In addition, this figure shows that the additional initial cost played a minute effect on the total cost. When the ASHP unit is changed for another with a higher rated power, the running cost difference between a traditional and modified ASHP would be larger, implying that more money could be saved by installing valves and trays in the multi-circuit outdoor coil due to improved operation performance and less energy consumed after modification. Thus, the modification of the multi-circuit outdoor coil should be fully considered when we design or optimize a bigger scale residential ASHP unit or commercial units (i.e. the rated heating capacity of the ASHP unit is higher than 6.5 kW).

In this study, the electricity unit price was assumed to be 0.9 CNY/kWh. Proportions of initial cost of the total cost over 15 operating years with electricity unit price variation from 0.7 to 1.1 CNY/kWh were discussed and presented in Fig. 13. As seen, the trend is decreasing as the electricity unit price increases. It is easy to understand that the operation cost is affected by the electricity price. At the same time, the difference of D6 and D4 is decreasing, from 0.83% with unit price at 0.7 CNY/kWh to 0.59% with unit price at 1.1 CNY/kWh. That means, as the electricity unit price increases, the additional initial cost effect on the total cost becomes smaller. If the electricity unit price decreases, we should also consider this modification with two reasons: 1) more energy could be saved with a higher rated power ASHP unit; and 2) environmental factor, more energy saved leads to a reduction in the environmental pollution. It is well known that environmental problem has a big negative influence on our life and society. Therefore, modifications should be fully considered no matter the unit price of electricity decreases or increases. This also demonstrates the fundamental meaning of this study.

4. Conclusions

A techno-economic analysis study on frosting/defrosting operations for an optimized ASHP unit, with trays and/or valves installed with its outdoor coil, was conducted and the results are reported. The following conclusions are made from this paper:

i. After the water collecting trays and/or valves were installed, economic performance of an ASHP unit was effectively improved. The total running cost decreased by as much as 3681.75 CNY, or 10.33%, the total cost 3516.75 CNY, or 4.67%, over 15 years of service life.
ii. After installing both the water collecting trays and valves, the running cost of the new ASHP unit in the heating season with frost formation decreased by 2540.36 CNY, or 11.95%, and in the heating season without frost formation the decrease was 1141.37 CNY, or 7.64%, over 15 years of service life.
iii. The effect of valves on economic performance of the ASHP unit is obviously better than that of trays. After water collecting trays were installed, the total cost decreased by 283.98 CNY. But the cost saved after the valves were installed enlarged 12.27 times, to 3484.34 CNY.
iv. The payback period for the additional initial cost was calculated at less than 8 months. Electricity unit price variation was further discussed. Contributions of this research work play important roles in application and evaluation of new technologies in the HVAC field.

Acknowledgments

The authors acknowledge the financial support from the National Natural Science Foundation of China (No. 51606044), Natural Science Foundation of Guangdong Province (No. 2017A030313300), and Science and Technology Planning Project of Guangdong Province, China (No. 2014B090903007) for the work reported in this paper. The first author is also grateful for the financial support of the Japan Society for the Promotion of Science (JSPS).

References

[1] T. Nishimura, Heat pumps-status and trends" in Asia and the Pacific, Int. J. Refrig. 25 (2002) 405–413.
[2] Y. Yao, Y.Q. Jiang, S.M. Deng, Z.L. Ma, A study on the performance of the airside heat exchanger under frosting in an air source heat pump water heater/chiller unit, Int. J. Heat Mass Transf. 47 (2004) 17–18.
[3] F.R. Ameen, J.E.R. Coney, C.G.W. Sheppard, Experimental study of warm-air defrosting of heat-pump evaporators, Int. J. Refrig. 16 (1993) 13–18.
[4] Y. Kim, A. Tikhonov, Y. Shin, J. Lee, Experimental study on high performance defrosting heater for household refrigerator, in: Proceedings of the 13th International Heat Conference, Sydney, Australia, 2006.
[5] R.M. Abdel-Wahed, M.A. Hifni, S.A. Sherif, Hot water defrosting of a horizontal flat plate cooling surface, Int. J. Refrig. 6 (1983) 152–154.
[6] H.J. Choi, B.S. Kim, D. Kang, K.C. Kim, Defrosting method adopting dual hot gas bypass for an air-to-air heat pump, Appl. Energy 88 (2011) 4544–4555.
[7] D. Wang, T. Tao, G. Xu, A. Luo, S. Kang, Experimental study on frosting suppression for a finned-tube evaporator using ultrasonic vibration, Exp. Thermal Fluid Sci. 36 (2012) 1–11.
[8] N. Sonobe, K. Fukiba, S. Sato, Y. Yoshimura, Method for defrosting heat exchangers using an air-particle jet, Int. J. Refrig. 60 (2015) 261–269.
[9] M.L. Qu, L. Xia, S.M. Deng, Y.Q. Jiang, A study of the reverse cycle defrosting performance on a multi-circuit outdoor coil unit in an air source heat pump. Part I: experiments, Appl. Energy 91 (2012) 122–129.
[10] K. Kwak, C. Bai, A study on the performance enhancement of heat pump using electric heater under the frosting condition heat pump under frosting condition, Appl. Thermal Eng. 30 (2010) 539–543.
[11] H. Factor, G.A. Grossman, A packed bed dehumidifier/regenerator for solar air-conditioning with liquid desiccants, J. Sol. Energy 24 (1980) 541–550.
[12] A.D. Sommers, A.M. Jacobi, Air-side heat transfer enhancement of a refrigerator evaporator using vortex generation, Int. J. Refrig. 28 (2005) 1006–1017.
[13] M.J. Song, D.M. Pan, N. Li, S.M. Deng, An experimental study on the negative effects of downwards flow of the melted frost over a multi-circuit outdoor coil in an air source heat pump during reverse cycle defrosting, Appl. Energy 138 (2015) 598–604.
[14] M.J. Song, S.M. Deng, D.M. Pan, N. Mao, An experimental study on the effects of downwards flowing of melted frost over a vertical multi-circuit outdoor coil in an air source heat pump on defrosting performance during reverse cycle defrosting, Appl. Thermal Eng. 67 (1–2) (2014) 258–265.
[15] E.U. Okoroafor, M. Newborough, Minimizing frost growth on cold surfaces exposed to humid air by means of crosslinked hydrophilic polymeric coatings, Appl. Thermal Eng. 20 (2000) 737–758.
[16] J.K. Dong, S. Li, Y. Yao, Y.Q. Jiang, Y. Tian, H. Tian, Defrosting performances of a multi-split air source heat pump with phase change thermal storage, Int. J. Refrig. 55 (2015) 49–59.
[17] M.J. Song, A.L. Chen, N. Mao, An experimental study on defrosting performance of an air source heat pump unit with a multi-circuit outdoor coil at different frosting evenness values, Appl. Thermal Eng. 94 (2016) 331–340.
[18] M.J. Song, N. Mao, S.M. Deng, Y.D. Xia, Y. Chen, An experimental study on defrosting performance for an air source heat pump unit at different frosting evenness values with melted frost locally drainage, Appl. Thermal Eng. 99 (2016) 730–740.
[19] M.J. Song, Z.H. Wang, N. Mao, Z. Li, Y. Chen, An experimental study on the uneven refrigerant distribution over a vertically installed multi-circuit outdoor coil in an ASHP unit during reverse cycle defrosting, Appl. Thermal Eng. 91 (2015) 975–985.
[20] M.J. Song, L. Xia, S.M. Deng, A modeling study on alleviating uneven defrosting for a vertical three-circuit outdoor coil in an air source heat pump unit during reverse cycle defrosting, Appl. Energy 161 (2016) 268–278.
[21] J.H. Kim, J.E. Braun, E.A. Groll, A hybrid method for refrigerant flow balancing in multi-circuit evaporators: upstream versus downstream flow control, Int. J. Refrig. 32 (2009) 1271–1282.
[22] M.J. Song, S.M. Deng, L. Xia, A semi-empirical modeling study on the defrosting performance for an air source heat pump unit with local drainage of melted frost from its three-circuit outdoor coil, Appl. Energy 136 (2014) 537–547.
[23] M.I. Hussain, A. Ali, G.H. Lee, Multi-module concentrated photovoltaic thermal system feasibility for greenhouse heating: model validation and techno-economic analysis, Sol. Energy 135 (2016) 719–730.
[24] M. Gustafsson, M.S. Gustafsson, J.A. Myhren, C. Bales, S. Holmberg, Techno-economic analysis of energy renovation measures for a district heated multi-family house, Appl. Energy 177 (2016) 108–116.
[25] P. Saban, H.E. Hasan, Techno-economic model for district heating systems, Energy Build. 72 (2014) 177–185.
[26] B. Giovanna, P. Antonio, G. Carolina, G. Iacopo, Techno-economic analysis of gas turbine inlet air cooling for combined cycle power plant for different climatic conditions, Appl. Thermal Eng. 82 (2015) 57–67.
[27] H.G. Syed Ihtsham, S.A. Mohd, T.B. Petrus, Energy saving technique for cooling dominated academic building: techno-economic analysis of its application, Appl. Energy 132 (2014) 192–199.
[28] K. Venkatesh, H. Kasun, H. Husnain, S. Rehan, Techno-economic performance evaluation of building cooling systems: A study of snow storage and conventional chiller systems, Cold Region Sci. Technol. 130 (2016) 8–20.
[29] S. Sau, N. Corsaro, T. Crescenzi, C. D'Ottavi, R. Liberatore, S. Licoccia, V. Russo, P. Tarquini, A.C. Tizzoni, Techno-economic comparison between CSP plants presenting two different heat transfer fluids, Appl. Energy 168 (2016) 96–109.
[30] Y.J. Ruan, Q.R. Liu, Z.W. Li, J.Z. Wu, Optimization and analysis of Building Combined Cooling, Heating and Power (BCHP) plants with chilled ice thermal storage system, Appl. Energy 179 (2016) 738–754.
[31] C.S. Antonio, R.A. Enrique, B.D. David, C.F. Eduardo, Evaluation of the cost of using power plant reject heat in low-temperature district heating and cooling networks, Appl. Energy 162 (2016) 892–907.
[32] A.R. Gurgel da Silva, C.E.T. Ortega, B.G. Rong, Techno-economic analysis of different pretreatment processes for lignocellulosic-based bioethanol production, Bioresour. Technol. 218 (2016) 561–570.
[33] H. Ali, A. Alireza, Techno-economic analysis of a PV/biomass/fuel cell energy system considering different fuel cell system initial capital costs, Sol. Energy 133 (2016) 409–420.
[34] W.T. Horton, E.A. Groll, J.E. Braun, Development of a High Performance Cold Climate Heat Pump, DOE-Purdue-0003842. 2014. (doi:10.2172/1133089).
[35] W. Wu, B.L. Wang, W.X. Shi, X.T. Li, Techno-economic analysis of air source absorption heat pump: Improving economy from a design perspective, Energy Build. 81 (2014) 200–210.
[36] M.J. Song, L. Xia, N. Mao, S.M. Deng, An experimental study on even frosting performance of an air source heat pump unit with a multi-circuit outdoor coil, Appl. Energy 164 (2016) 36–44.